ARTICLE NO. 78-486

Probability of Solid-Propellant Motor Failure Due to Environmental Temperatures

R.A. Heller,* M.P. Kamat,† and M.P. Singh†
Virginia Polytechnic Institute and State University, Blacksburg, Va.

Solid-propellant rocket motors are frequently stored in the field without environmental protection; hence they are subjected to variable thermal stresses and material degradation due to aging and fatigue. Temperature variations are modeled as narrow-band random processes; thermal stresses in the motor will exhibit similar characteristics. Because material properties are statistically distributed, the probability that the thermal stress exceeds the strength of the propellant is synonymous with the probability of failure. A simplified solid-propellant rocket motor is analyzed as a long hollow elastic cylinder in a thin case (plane strain). The daily probabilities of failure are determined from a stress-strength interference-type analysis as functions of time and are summed up to produce the probability of failure at the end of the service life. The additional complexities of viscoelasticity, aging, and loads other than thermal will be introduced in subsequent analyses.

Nomenclature

A,a = random amplitude
a = r_1, radius of bore
$a(t)$ = $\cos 2\pi f_y t$
A_j = constant of integration
b = r_2, outer radius of propellant
B_j = constant of integration
c = r_3, outer radius of casing
c_j = specific heat, Btu/lb$_m$ °F (J/kg°C)
D,d = random peak diurnal temperature
$E(x^2)$ = mean-square value
E_j = modulus of elasticity, psi (N/m^2)
$f;f_y,f_d$ = frequency (cy/h); for annual and daily wave
$f_X(x)$ = probability density function
$F_X(x)$ = cumulative distribution function
i = $\sqrt{-1}$
j = index for motor layers, $j=1,\ldots,4$
k = index for stress component, $k=r,\theta$
k_j = thermal conductivity, Btu/in. h°F (W/m °C)
$L_X(x);L_1,L_n$ = reliability function; for one application, for n applications
p' = interfacial pressure
P = probability
$P_f;P_{f_1},P_{f_n}$ = probability of failure; for one application, for n applications
r,r_j = radius
$r_s,R_s;r_{s_c}$ = radom strength; characteristic value of Weibull distribution, psi (N/m^2)
$R_j(r,f)$ = frequency response function of temperature
$s,S;s_y,S_y,s_d,S_d$ = random stress; due to seasonal and diurnal cycle
S_r,S_θ,S_z = stress components
t = time
$T(t)$ = time-dependent part of solution
$U,U_j;U_{\text{in}},U_o,$ U_y,U_d,U_f = temperature °F (°C); input, output, annual, daily, and stress free
$W_{\text{in}};W_o$ = power spectrum; input, output
x_j = $r\sqrt{2\pi f_y/\alpha_j}$
y,Y = random peak annual temperature
α_j = thermal diffusivity, in.^{2}/h (m^2/s)
$\bar{\alpha}_j$ = thermal coefficient of expansion, in./in./°F (m/m/°C)
β_{r_s} = Weibull shape parameter for strength
$\Delta\nu_s,\Delta\nu_\epsilon$ = safety range
∂ = differential
$\epsilon_r,\epsilon_\theta$ = strain components
ϕ_j = phase angle
μ_y,μ_U = annual mean temperature, mean temperature change
$\mu_p',\mu_s',\mu_\epsilon'$ = mean pressure, mean stress, mean strain
ν_j = Poisson's ratio
π = 3.14
ρ_j = mass density, lb-s^2/in.^{4} (kg/m^3)
$\sigma;\sigma_y,\sigma_d$ = standard deviation; for annual peak, for diurnal peak

Introduction

In a series of papers[1-4] published during the last two years, the development of a probabilistic life prediction methodology for solid rocket motors has been proposed. The geometry of actual motors is quite complicated, and the propellant consists of load-rate- and temperature-dependent viscoelastic materials. For the sake of tractability, several simplifying assumptions have been made. Hence motors have been modeled as long hollow elastic cylinders (plane strain) encased in a thin steel casing and an insulated container.[4] They were subjected to environmental temperature variations, which in turn produced thermal stresses and strains in the propellant.[3,4] Large thermal stress gradients induced by rapid temperature changes and extreme thermal conditions may produce stresses and/or strains in excess of the strength and/or strain capacity of the material. For real motors the latter two properties are also temperature and rate dependent but, again for simplicity, will be assumed independent here.

Because both thermal load and material properties are statistically variable quantities, the probability of failure is calculated on the basis of stress strength interference principles.[3,4] In this paper only the statistical variability of the strength and strain capacity are considered, while the statistics of other mechanical and thermal properties are neglected. The

Presented as Paper 78-486 at the AIAA/ASME 19th Structures, Structural Dynamics, and Materials Conference, Bethesda, Md., April 3-5, 1978; submitted May 17, 1978; revision received Nov. 16, 1978.

Index categories: Solid and Hybrid Rocket Engines; Reliability, Maintainability, and Logistics Support; LV/M Structural Design (including Loads).

*Professor of Engineering Science and Mechanics. Associate Fellow AIAA.

†Associate Professor of Engineering Science and Mechanics.

probability of failure increases with time and eventually makes the motor unserviceable, hence leading to a storage life definition.[3,4]

In previous reports idealized representations of thermal power spectra were used. The temperature was assumed to consist of an annual mean and a deterministic (constant-amplitude) seasonal cycle with all random variations attributed to the diurnal temperature change. Furthermore, the power spectrum around the diurnal frequency was considered to consist of a narrow rectangle. Additionally, all material properties were assumed to be elastic and normally (statistically) distributed.

The present paper still utilizes elastic material properties but considers the more realistic Weibull distribution as the statistical model, and thermal loads are calculated with the use of actual, measured, power spectra.

Random processes can be treated either in the time domain or in the frequency domain. In the first case the input (temperature) and resulting output (stress, strain) are time series, usually in the form of Fourier series. In order to obtain probability distributions of the output, a large number of input functions are used in a Monte Carlo simulation technique.[5,6]

The second approach, employed in this paper, utilizes a particular frequency decomposition of the input time series, the so-called power spectrum. As a result, power spectra are obtained for the output quantities, which allow calculation of statistical parameters directly.[1,2,4]

Transient Heat Transfer in an Insulated, Case-Bonded Cylinder

To determine the response of an insulated, case-bonded, hollow propellant cylinder to a randomly varying temperature input in the absence of wind and radiation, first the steady-state transient heat transfer problem has to be solved.

The Fourier heat conduction equation applied to a long, axisymmetric, layered cylinder, shown in Fig. 1, is solved for the temperature $U_j(r,t)$ in the jth layer[7]:

$$\frac{\partial^2 U_j}{\partial r^2} + \frac{1}{r}\frac{\partial U_j}{\partial r} = \frac{1}{\alpha j}\frac{\partial U_i}{\partial j} \qquad (j=1,2,\ldots,n) \qquad (1)$$

The temperature $U_j(r,t)$ is a function of both the radial coordinate r and the time t, with α_j the thermal diffusivity of the jth layer in in.^{2}/h or m^2/s.

The j differential equations are subject to the following boundary conditions: 1) the temperature at the center of the cylinder must be finite; 2) the temperatures on both sides of an interface must be identical; 3) the heat flux across an interface must be continuous; and 4) the temperature of the outer surface undergoes a sinusoidal variation with unit amplitude and frequency f. For a four-layer cylinder, four second-order differential equations and hence eight boundary conditions are required.

B.C. 1: $U_1(0,t) = \text{finite}$

B.C. 2,3,4: $U_j(r_j,t) = U_{j+1}(r_{j+1},t) \quad (j=1,2,3)$

B.C. 5,6,7: $k_j \dfrac{\partial U_j(r_j,t)}{\partial r} = k_{j+1}\dfrac{\partial U_{j+1}(r_{j+1},t)}{\partial r} \quad (j=1,2,3)$

B.C. 8: $U_4(r_4,t) = e^{i(2\pi ft)}$

where the thermal diffusivities, α_j are given as $\alpha_j = k_j/\rho_j c_j$. The solution of the differential equation, Eq. (1), is obtained by separation of variables:

$$U_j(r,t) = R_j(r,f)\,T(t) \qquad (2)$$

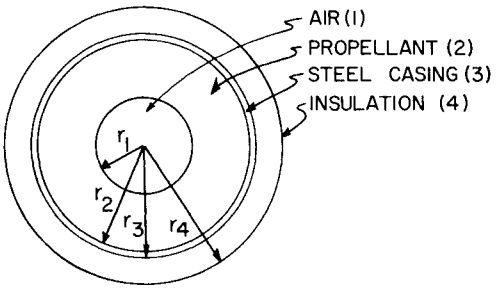

Fig. 1 Layered cylinder.

where $R_j(r,f)$, the space- and frequency-dependent part of the solution, is the so-called frequency response function. $R_j(r,f)$ may be written in terms of complex Kelvin functions[2,8] as

$$R_j(r,f) = A_j(\text{ber}\,x_j + i\,\text{bei}\,x_j) + B_j(\text{ker}\,x_j + i\,\text{kei}\,x_j) \qquad (3)$$

with

$$x_j = \sqrt{2\pi f/\alpha_j} \qquad (4)$$

Substitution of the eight boundary conditions into Eq. (3) results in seven linear equations from which seven of the coefficients of Eq. (3) may be evaluated while boundary condition 1 requires that $B_1 = 0$ because ker x_j at $x=0$ is unbounded.

The real and imaginary components of the frequency response function $R_j(r,f)_{\text{Re}}$ and $R_j(r,f)_{\text{Im}}$ given by Eq. (2) yield an absolute value $|R_j(r,f)|$ and a phase angle ϕ_j. Consequently, Eq. (2) may also be expressed as

$$U_j(r,t) = |R_j(r,f)|\exp[i(\phi_j + 2\pi ft)] \qquad (5)$$

Characterization of Random Environmental Temperatures

In order to analyze environmental temperature as a random variable, a long time series (10 years) of hourly temperature measurements, typical for the southwestern United States, was examined.[9] First the 10-year mean value, μ_y was extracted. The remaining time series, now with zero mean, was next subjected to a fast Fourier transform (FFT) analysis in order to obtain its power spectral representation. The resultant spectrum, which is essentially a frequency decomposition of the time series, consists of several peaks, as seen on Fig. 2, with power plotted on a log scale. The total area under the complete power spectrum is equal to the variance of the series (with zero mean).[10]

An examination of the spectrum, plotted on a natural scale as shown in Fig. 3, indicates two predominant peaks centered around the frequencies of the seasonal and diurnal cycles. The heights of these two peaks are two orders of magnitude greater than all other peaks. Furthermore, the areas under them account for 88% of the total variance. Integration was carried out numerically. Limits of integration were selected so that integration would be discontinued if the added area was less than 0.1% of the accumulated area.

On the basis of these facts, it is reasonable to assume that temperature is a pseudorandom variable that consists of the sum of two narrow-band excitations whose amplitudes and frequencies have statistical variations, as indicated schematically in Fig. 4. It is common experience that peak diurnal temperatures vary and are not exactly 24 h apart on consecutive days. Hence the diurnal peak, centered over the 1/24-h frequency represents a narrow-band, pseudocyclic phenomenon. A similar argument can be advanced for the seasonal peak.

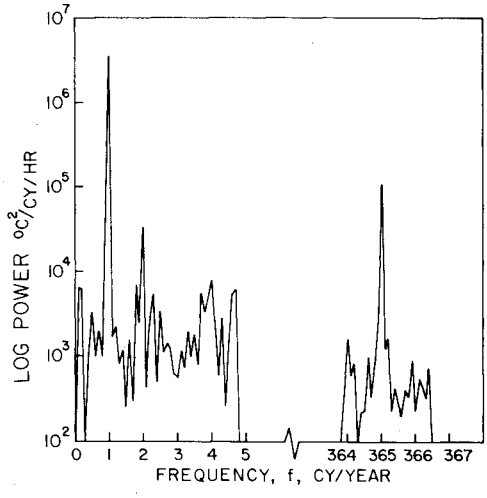

Fig. 2 Power spectral density (log scale).

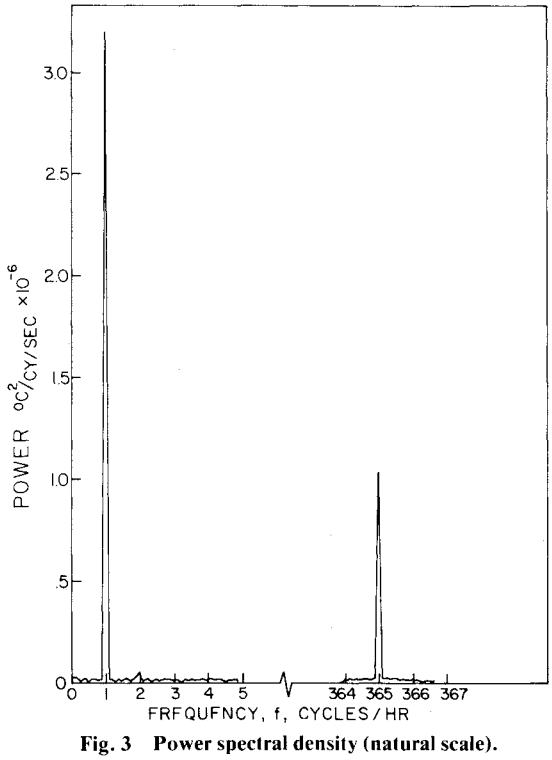

Fig. 3 Power spectral density (natural scale).

When stationary random process theory is utilized, the mean square of the temperature is equal to the area under the power spectrum:

$$E(U_{\text{in}}{}^2) = \int_0^\infty W_{\text{in}}(f)\,df \tag{6}$$

where $W_{\text{in}}(f)$ is the input power spectral density in deg²/cy/h.

On the other hand the output power spectral density of the temperature in the interior of the motor may be calculated with the aid of the frequency response function:

$$W_o(r,f) = |R_j(r,f)|^2 W_{\text{in}}(f) \tag{7}$$

The variance of the temperature at an internal point is obtained analogously to Eq. (6):

$$E[U_{j_0}(r)^2] = \int_0^\infty W_{j_0}(r,f)\,df = \int_0^\infty |R_j(r,f)|^2 W_{\text{in}}(f)\,df \tag{8}$$

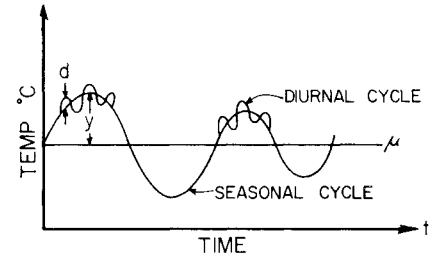

Fig. 4 Schematic temperature model.

If the temperature is modeled as the superposition of two narrow-band stationary processes, and the small areas not included within the narrow frequency ranges f_1 to f_2 and f_3 to f_4 are apportioned to the two peaks so that their combined areas add up to the total area under the original power spectrum, the variances of the annual and diurnal waves may be approximated as

$$E(U_y^2) = \int_{f_1}^{f_2} W_{\text{in}}(f)\,df \tag{9}$$

and

$$E(U_d^2) = \int_{f_3}^{f_4} W_{\text{in}}(f)\,df \tag{10}$$

The variances of the output are determined analogously to Eq. (8), with appropriate limits of integration.

The average frequency of a narrow-band process may also be calculated from the power spectrum.[10] For the annual output wave, for instance,

$$\bar{f}_y^2 = \int_{f_1}^{f_2} f^2 |R(r,f)|^2 W_{\text{in}}(f)\,df / E(U_{yo}^2) \tag{11}$$

Distribution of Amplitudes

According to random process theory, a narrow-band process, whose magnitudes follow a Gaussian (normal) distribution, when transmitted through linear differential equations produces an output that is also narrow band and has a Gaussian magnitude distribution.

Additionally, it can be proven[9] that the amplitudes of a Gaussian narrow-band signal with zero mean follow the Rayleigh distribution, whose probability density function is given as[11]

$$f_A(a) = \frac{a}{\sigma^2}\exp\left[-\frac{1}{2}\left(\frac{a}{\sigma}\right)^2\right] \tag{12}$$

where a is a value of the amplitude A and σ is the standard deviation of the underlying Gaussian process, i.e., the square root of the variance. The probability that an amplitude greater than a is encountered can be obtained by integration of Eq. (12):

$$P(A>a) = \int_a^\infty \frac{a}{\sigma^2}\exp\left[-\frac{1}{2}\left(\frac{a}{\sigma}\right)^2\right]da = \exp\left[-\frac{1}{2}\left(\frac{a}{\sigma}\right)^2\right] \tag{13}$$

Other studies indicate[9] that when temperatures are considered as the sum of daily and seasonal effects, each of these can be approximated by normal distributions. Hence the assumption of normality is reasonable.

To arrive at the distribution of the minimum temperatures for each day of the year, the amplitude of the daily wave D, which is Rayleigh distributed, is added to a cosine wave with an effective frequency f_y and the amplitude of the seasonal cycles Y, which is also Rayleigh distributed, all superimposed on an annual mean temperature μ_y (Fig. 4):

$$U = \mu_y + Ya(t) + D \tag{14}$$

where $a(t) = \cos 2\pi f_y t$.

The density function of the minimum daily temperature is obtained as a convolution integral:

$$f_U(U) = \frac{1}{|a|}\int_{-\infty}^{\infty} f_y\left(\frac{U-\mu_y-D}{a}\right) f_D(D)\,\mathrm{d}D \qquad (15)$$

Because the two amplitudes, Y and D, may theoretically range from 0 to $+\infty$ while $-1<a<1$, the integration indicated in Eq. (15) is carried out separately for the positive and negative values of $a(t)$ and has to be performed for each day of the year. A detailed derivation of Eq. (15) is found in Ref. 12.

Transient Thermal Stresses and Strains

The distribution of thermal stresses and strains in a case-bonded hollow cylinder under plane strain conditions (long cylinder) have been developed in Refs. 4 and 13 for arbitrary temperatures. Those relations will be used here for the case of a sinusoidal surface temperature input. The frequency response functions for radial and circumferential stresses in the propellant are written as

$$S_r(r,f) = -\frac{b^2p'}{b^2-a^2}\left(1-\frac{a^2}{r^2}\right) + \frac{\bar{\alpha}_2E_2}{(1-\nu_2)(b^2-a^2)} \times\left(1-\frac{a^2}{r^2}\right)\int_a^b R_2(r,f)r\mathrm{d}r - \frac{\bar{\alpha}_2E_2}{(1-\nu_2)r^2}\int_a^r R_2(r,f)r\mathrm{d}r \qquad (16)$$

$$S_\theta(r,f) = -\frac{b^2p'}{b^2-a^2}\left(1-\frac{a^2}{r^2}\right) + \frac{\bar{\alpha}_2E_2}{(1-\nu_2)(b^2-a^2)} \times\left(1-\frac{a^2}{r^2}\right)\int_a^b R_2(r,f)r\mathrm{d}r + \frac{\bar{\alpha}_2E_2}{(1-\nu_2)r^2}\int_a^r R_2(r,f)r\mathrm{d}r - \frac{\bar{\alpha}_2E_2R_2(r,f)}{1-\nu_2} \qquad (17)$$

where

$$p' = \frac{E_2E_3\left[2\bar{\alpha}_2(1+\nu_2)\int_a^b R_2(r,f)r\mathrm{d}r - \bar{\alpha}_3(1+\nu_3)(b^2-a^2)R_2(b,f)\right]}{\{E_3(1+\nu_2)[(1-2\nu_2)b^2+a^2]+E_2(1-\nu_3^2)b[(b^2-a^2)/(c-b)]\}} \qquad (18)$$

with E_j, $\bar{\alpha}_j$, and ν_j the moduli of elasticity, thermal coefficients of expansion, and Poisson's ratios for propellant ($j=2$) and casing ($j=3$); $R_2(r,f)$ is the temperature frequency response function of Eq. (3).

Similarly the frequency response functions for radial and circumferential strain components are given:

$$\epsilon_r(r,f) = -\frac{(1+\nu_2)b^2p'}{E_2(b^2-a^2)}\left[(1-2\nu_2)-\frac{a^2}{r^2}\right] + \frac{(1+\nu_2)\bar{\alpha}_2}{(1-\nu_2)(b^2-a^2)}\left[(1-2\nu_2)-\frac{a^2}{r^2}\right]\int_a^b R_2(r,f)r\mathrm{d}r - \frac{\bar{\alpha}_2(1+\nu_2)}{(1-\nu_2)r^2}\int_a^r R_2(r,f)r\mathrm{d}r + \frac{1+\nu_2}{1-\nu_2}\bar{\alpha}_2R_2(r,f) \qquad (19)$$

and

$$\epsilon_\theta(r,f) = -\frac{(1+\nu_2)b^2p'}{E_2(b^2-a^2)}\left[(1-2\nu_2)+\frac{a^2}{r^2}\right] + \frac{(1+\nu_2)\bar{\alpha}_2}{(1-\nu_2)(b^2-a^2)}\left[(1-2\nu_2)+\frac{a^2}{r^2}\right]\int_a^b R_2(r,f)r\mathrm{d}r + \frac{(1+\nu_2)\bar{\alpha}_2}{(1-\nu_2)r^2}\int_a^r R_2(r,f)r\mathrm{d}r \qquad (20)$$

The variances are obtained, as in Eq. (8) and subsequent relations, by replacing $|R_j(r,f)|^2$ with the appropriate frequency response function for stress or strain. The variances due to the annual wave, for instance, become

$$E[S_{k_y}^2(r)] = \int_{f_1}^{f_2} |S_k(r,f)|^2 W_{\text{in}}(f)\,\mathrm{d}f \qquad (k=4,\theta) \qquad (21)$$

and

$$E[\epsilon_{k_y}^2(r)] = \int_{f_1}^{f_2} |\epsilon_k(r,f)|^2 W_{\text{in}}(f)\,\mathrm{d}f \qquad (k=r,\theta) \qquad (22)$$

while those for the daily wave are calculated by integrating from f_3 to f_4.

By using the appropriate stress or strain frequency response functions in Eq. (11), average frequencies will result.

Stresses and Strains Due to Uniform Temperature

Stresses and strains produced by a uniform temperature through the web of the motor may be obtained from Eqs. (16-21) by substituting

$$\mu_U = -(U_f-\mu_y) \qquad (23)$$

for $R_2(r,f)$. Here U_f is the strain-free temperature, the temperature at which the propellant was cast, and μ_y is the annual mean tempeature.

$$\mu'_{s_r}(r) = -\frac{b^2\mu_p}{b^2-a^2}\left(1-\frac{a^2}{r^2}\right) \qquad (24)$$

$$\mu'_{s_\theta}(r) = -\frac{b^2\mu_p}{b^2-a^2}\left(1+\frac{a^2}{r^2}\right) \qquad (25)$$

$$\mu'_{\epsilon_r}(r) = -\frac{(1+\nu_2)b^2\mu_p}{E_2(b^2-a^2)}\left[(1-2\nu_2)-\frac{a^2}{r^2}\right] + (1+\nu_2)\bar{\alpha}_2\mu_U \qquad (26)$$

Table 1 Physical parameters

Stress-free temperature, $U_f = 71°C$
Mean temperature, $\mu_y = 23°C$
Temperature standard deviation, $\sigma = 9.77°C$
Diffusivity of air, $\alpha_1 = 1.915\times10^{-5}$ m^2/s
Diffusivity of propellant, $\alpha_2 = 2.412\times10^{-7}$ m^2/s
Diffusivity of casing, $\alpha_3 = 8.770\times10^{-6}$ m^2/s
Thermal conductivity of air, $k_1 = 2.45\times10^{-2}$ W/m °C
Thermal conductivity of propellant, $k_2 = 4.09\times10^{-1}$ W/m °C
Thermal conductivity of casing, $k_3 = 2.53\times10^{1}$ W/m °C
Radius of cavity, $a = 0.064$ m
Outer radius of propellant, $b = 0.201$ m
Outer radius of casing, $c = 0.203$ m
Modulus of elasticity for propellant, $E_2 = 1.72\times10^6$ N/m^2
Modulus of elasticity for casing, $E_3 = 2.07\times10^{11}$ N/m^2
Poisson's ratio for propellant, $\nu_2 = 0.49$
Poisson's ratio for casing, $\nu_3 = 0.25$
Coefficient of thermal expansion for propellant, $\alpha_2 = 3.3\times10^{-5}$ m/m/°C
Coefficient of thermal expansion for casing, $\alpha_3 = 3.6\times10^{-6}$ m/m/°C
Strength characteristic value for propellant, $r_{s_c} = 3.36\times10^6$ N/m^2
Shape parameter for propellant, $\beta_r = 10$

$$\mu'_{\epsilon_\theta} = -\frac{(1+\nu_2)b^2\mu_p}{E_2(b^2-a^2)}\left[(1-2\nu_2)+\frac{a^2}{r^2}\right]+(1+\nu_2)\bar{\alpha}_2\mu_U \tag{27}$$

with

$$\mu_p = \frac{\{E_2E_3(b^2-a^2)\,[\bar{\alpha}_2(1+\nu_2)-\bar{\alpha}_3(1+\nu_3)\,]\mu_U\}}{\{E_3(1+\nu_2)\,[\,(1-2\nu_2)b^2+a^3\,]+E_2(1+\nu_3^2)b[\,(b^2-a^2)/(c-b)\,]\,\}} \tag{28}$$

Statistical Distributions of Strength, Strain Capacity, Stress, and Strain

As discussed in the Introduction, the tensile strength and strain capacity of engineering materials are statistically variable quantities. Examination of test results for propellants at constant temperatures and strain rates indicates that both the ultimate tensile strength and strain capacity are well represented by the Weibull distribution. Because in this presentation the materials are assumed to be elastic, temperature and rate effects are not considered.

The probability that the ultimate strength of the material R_s is greater than a given value r_s is written as

$$L_{R_s}(r_s) = P(R_s > r_s) = \exp[-(r_s/r_{s_c})^{\beta_{r_s}}] \tag{29}$$

where β_{r_s} is the shape parameter and r_{s_c} is the characteristic value of the distribution. Identical expressions may be written for strain capacity in terms of the shape parameter β_{r_ϵ} and characteristic value r_{ϵ_c}.

It has been explained that Gaussian (normal) inputs when applied to linear systems produce Gaussian outputs and that the distribution of peaks is of the Rayleigh type. Consequently, the difference between the strain-free temperature and the sum of the annual mean temperature and two narrow-band temperature processes, seasonal and diurnal, produce stresses and strains with underlying Gaussian distributions and Rayleigh peak distributions. As a result, Eqs. (12) and (13) are also applicable to the evaluation of the density functions for stresses and strains.

The maximum daily stress (strain) at any point in the interior of the propellant layer is expressed analogously to the temperature [Eq. (14)] as

$$S_k(r,t) = \mu_{S_k}(r) + S_{y_k}(r)a(t) + S_{d_k}(r) \tag{30}$$

where $\mu_{S_k}(r)$ is the stress produced by the temperature difference between the stress-free temperature and the annual mean [Eqs. (24-30)], $S_{y_k}(r)$ and $S_{d_k}(r)$ are the Rayleigh-distributed stress amplitudes due to the seasonal and diurnal cycles, and $a(t) = \cos 2\pi f_y t$.

The probability density function of daily stress peaks becomes equal to

$$f_{S_k}(s_k) = \frac{1}{|a|}\int_{-\infty}^{\infty} f_{S_y}\left(\frac{s_k-\mu_{s_k}-s_{d_k}}{a}\right) f_{S_d}(s_{d_k})\,ds_{d_k} \tag{31}$$

with $f_{S_{y_k}}(s_y)$ and $f_{S_{d_k}}(s_d)$ the appropriate Rayleigh distributions. The detailed intergration of Eq. (31) is found in Ref. 12.

The Probability of Failure

The safety range, as defined in structural analysis, is the difference between the strength (strain capacity) of the material and the applied stress (strain)[3]:

$$\Delta\nu_s = R_s - S \tag{32}$$

and

$$\Delta\nu_\epsilon = R_\epsilon - \epsilon \tag{33}$$

where $\Delta\nu_s$ and $\Delta\nu_\epsilon$ are the safety ranges for stress and strain, respectively, while R_s and R_ϵ are the strength and strain capacity of the material. Since R_s and S, as well as R_ϵ and ϵ, are random variables, the safety ranges are random variables likewise.

For viscoelastic propellants, failure criteria involve temperature and strain-rate-dependent states of stress and strain, leading to more complicated failure conditions. For an elastic material considered in the present analysis, however, the motor will fail if either the strength or the strain capacity is exceeded by the maximum applied stress or the maximum strain, respectively; that is if either

$$\Delta\nu_s \le 0 \tag{34}$$

or

$$\Delta\nu_\epsilon \le 0 \tag{35}$$

In the case of a solid-propellant rocket motor, the temperature difference between the strain-free temperature and ambient conditions is always negative. As a result the greatest tensile stress component is either the tangential stress at the bore or the radial interfacial stress, while the largest tensile strain is the tangential strain component at the bore. Consequently, the probability of failure P_{f_1}, under a single load application, is synonymous with the probability that $\Delta\nu_{S_\theta}(r_1)$, $\Delta_{S_r}(r_3)$, or $\Delta\nu_{\epsilon_\theta}(r_1)$ are equal to or less than zero which is expressed as the union of the events. Because the probability that two types of failure will occur simultaneously is highly unlikely, the union is approximated (conservatively) by the sum of probabilities:

$$P_{f_1} = P_{f_{S_{\theta_1}}} + P_{f_{\epsilon_{\theta_1}}} + P_{f_{S_{r_1}}} \tag{36}$$

The reliability of the motor for one-load application is equal to

$$L_1 = 1 - P_{f_1} \tag{37}$$

while for n repeated loads, using the multiplication rule of probabilities, the probability of surviving all of them is given as an n-fold product:

$$L_n = \prod_{i=1}^{n}[1-P_{f_1}(n)] \tag{38}$$

where $P_{f_1}(n)$ is the probability of failure during the nth application of the load.[3] When the $P_{f_1}(n)$ terms are small, the product of Eq. (38) may be replaced by the more conservative approximation

$$L_n = 1 - \sum_{i=1}^{n} P_{f_1}(n) \tag{39}$$

The probability of failure for n load repetitions is therefore expressed as

$$P_{f_n} = \sum_{i=1}^{n} P_{f_1}(n) \tag{40}$$

Real propellants are subject to cumulative damage as well as aging due to repeated and sustained loads and temperatures. However, again for the sake of tractability, neither of these two cases will be included in the present analysis.

Since it is assumed that the annual temperature cycle and hence the stress and strain cycles are repetitive, it is sufficient to carry out the summation indicated in Eq. (39) for a single pseudoyear. To determine the probability of failure of a motor at the end of a service life of N years, the pseudoannual probability

$$P_f(T_y) = \sum_{i=1}^{T_y} P_f(n) \tag{41}$$

where $T_y = f_d/f_y$ pseudodays per pseudoyear, is simply multiplied by $8760 f_y N$. Therefore

$$P_f = 8760 f_y N P_f(T_y) \tag{42}$$

Thus the service life of a motor may be calculated for a chosen probability of failure. The probability terms of Eq. (36) are individually calculated as

$$P_{f_{s_{\theta_1}}} = P(\Delta\nu_{s_\theta} \le 0) = P[(R_s - S_\theta) \le 0] \tag{43}$$

The probability density function of the difference of two random variables is a convolution integral, and the probability that this difference is less than zero may be written as[3]

$$P_{f_{s_{\theta_1}}} = \int_0^\infty F_{R_s}(s_\theta) f_{s_\theta}(s_\theta)\, ds_\theta \tag{44}$$

where $F_{R_s}(s_\theta)$ is the probability that the strength R_s is less than the stress s_θ and is given by Eq. (29)

$$F_{r_s}(s_\theta) = 1 - L_{R_s}(s_\theta) = 1 - \exp[-(s_\theta/r_{s_c})^{\beta_{r_s}}] \tag{45}$$

and $f_{s_\theta}(s_\theta)$ is obtained from Eq. (31). Using these relations the probability of failure

$$P_{f_{s_1}} = \int_{\mu_{s_\theta}}^\infty \{1 - \exp[-(S_k/r_c)^{\beta_r}]\} f_{S_k}(s_k)\, dS_k \quad (0 < a) \tag{46}$$

or

$$P_{f_{s_1}} = \int_{-\infty}^\infty \{1 - \exp[-(S_k/r_c)^{\beta_r}]\} f_{S_k}(s_k)\, dS_k \quad (a < 0) \tag{47}$$

with the appropriate density functions. The other two terms of Eq. (36) are calculated analogously, and the total probability of failure for N years is computed from Eq. (42).

Application to Solid-Propellant Motor

The relationships discussed in the previous sections have been utilized to evaluate the probability of failure and the expected storage life of a solid-propellant motor for environmental conditions typical of the southwestern United States. Mechanical, thermal, and geometric properties of the motor are presented in Table 1.

The power spectrum of temperatures, derived from temperature records obtained from the U.S. Department of Commerce,[14] was considered to consist of two distinct peaks from which the effective frequencies of the seasonal and diurnal cycles were calculated as [Eq. (11)] $f_y = 1.16 \times 10^{-4}$ cy/h (360 days/year) and $f_d = 4.16 \times 10^{-2}$ cy/h (24.04 h/day). When utilizing the Rayleigh distribution of temperature amplitudes [Eq. (12)] and the standard deviations

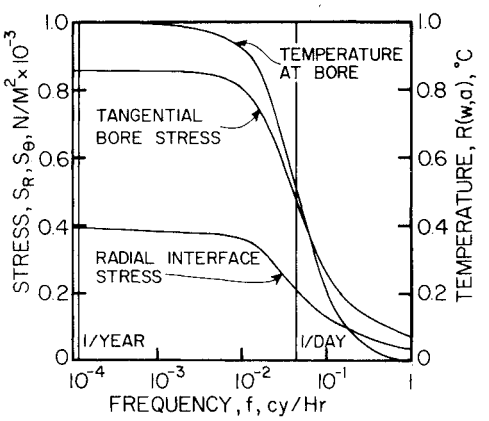

Fig. 5 Frequency response functions.

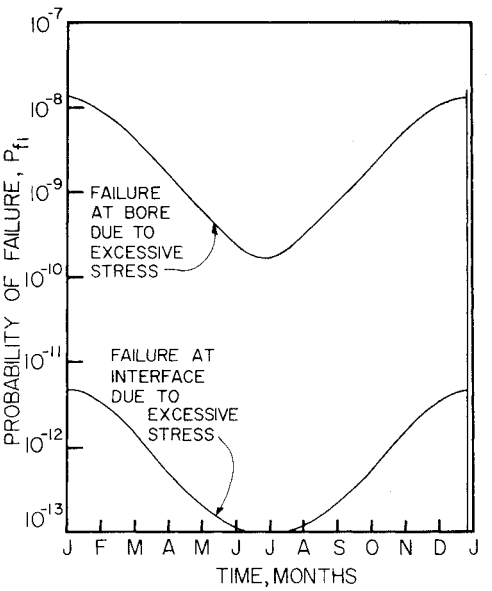

Fig. 6 Daily probabilities of failure.

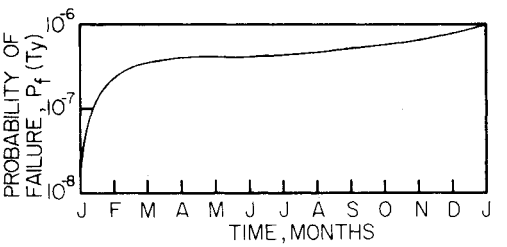

Fig. 7 Progressive probability of failure.

for the above two waves: $\sigma_y = 8.00$ °C and $\sigma_D = 4.47$ °C calculated from Eqs. (9) and (10), the average amplitude of the seasonal and diurnal cycles were found to be[10] $\bar{y} = 1.25\ \sigma_y = 10.00$ °C and $\bar{D} = 1.25\ \sigma_D = 5.59$ °C, respectively.

Next the frequency response function for the temperature at the bore of an uninsulated cylinder was evaluated with the aid of Eq. (3) and the boundary conditions B.C. 1-B.C. 8; it is shown in Fig. 5. It is evident that for low frequencies the temperature distribution through the web is uniform, considering that the casing is subjected to a unit amplitude thermal cycle. For high frequencies the interior of the cylinder remains unaffected, resulting in significant thermal gradients in the web. Frequency response functions are also shown for the tangential stress component at the bore and the radial stress at the interface between propellant and casing. It is seen

from the figure that low-frequency thermal cycles produce high stresses at these two critical locations.

The probability of failure for each day of the year has been determined both at the bore and at the interface, as presented in Fig. 6. The probability of failure is greatest in the winter when the difference between the stress-free temperature and ambient conditions is largest.

Failure under repeated loading is calculated as the sum of the daily probabilities based on Eq. (41) (Fig. 7). This relationship assumes that the temperature on any day is independent of conditions on the preceding day. Such a simplification has been necessary in order to manage an already complicated problem. The assumption leads to a conservative (higher) estimate for the probability of failure. At the end of the first year a probability of failure, $P_f(T_y) = 10^{-6}$ is reached. It is further assumed that loading is repeated annually until an unacceptably high probability of failure of say one in a hundred thousand is reached. Hence a service life of 10 years is stipulated.

Conclusions

A probabilistic service life prediction methodology has been presented for solid-propellant rocket motors subjected to environmental temperatures. In its present form the technique considers an elastic material without aging, cumulative damage, or viscoelastic properties and does not consider the effects of solar radiation. These additional inputs are currently being applied to a more refined model.

Acknowledgments

The work presented here has been performed under Contract No. DAAH01-C-76-1070. The authors wish to acknowledge the cooperation of the Project Engineer, T.H. Duerr of Redstone Arsenal.

References

[1] Heller, R.A., "Temperature Response of an Infinitely Thick Slab to Random Surface Temperatures," *Mechanics Research Communications,* Vol. 3, No. 5, 1976, pp. 379-385; also, U.S. AMICOM TR.RK-76-13, May 6, 1976.

[2] Heller, R.A., "Thermal Stress as a Narrow-Band Random Load," American Society of Civil Engineers, EM5, No. 12450, Oct. 1976, pp. 787-805; also, U.S. AMICOM. TR.RK-7T-1, May 7, 1976.

[3] Heller, R.A., "Life Prediction of Dump Stored Motors with Statistically Varying Strength and Temperature," U.S. Army Missile Command, TR. RK-76-12, April 1976.

[4] Heller, R.A. and Kamat, M.P., "Probabilistic Life Prediction for Rocket Motors Subjected to Random Thermal Loads," Chemical Propulsion Information Agency, 14th JANNAF Structures and Mechanical Working Group Meeting, Laurel, Md., CPIA Report No. 283, Feb. 15-17, 1977.

[5] Cost, T.L., "Probabilistic Service Life Prediction of Solid Rocket Motors Subjected to Thermal Load Using Computer Simulation," Chemical Propulsion Information Agency, 14th JANNAF Structures and Mechanical Working-Group Meeting, Laurel, Md., CPIA Report No. 283, Feb. 15-17, 1977.

[6] Cost, T.L., "Computer Simulated Thermo-Structural Response of Composite Cylinders Due to Random Thermal Environments," *Procedings of Conference of Environmental Degradation of Engineering Materials,* Virginia Polytechnic Institute, Blacksburg, Va., Oct. 10-12, 1977.

[7] Eckert, E.R.G. and Drake, R.M., *Heat and Mass Transfer,* McGraw Hill, New York, 1959, p. 97.

[8] Abramovitz, M. and Stegun, I.A., *Handbook of Mathematical Functions,* National Bureau of Standards, Applied Mathematics Series 55, 1964, pp. 379-385.

[9] Essenwanger, O. and Dudel, H., Physical Sciences Branch, Redstone Arsenal, Ala., private communication, 1976.

[10] Crandall, S.H., *Random Vibration in Mechanical Systems,* Academic Press, New York, 1963, p. 71.

[11] Hahn, J.G. and Shapiro, S.S., *Statistical Models in Engineering,* Wiley, New York, 1977, pp. 131-132.

[12] Heller, R.A. and Singh, M.P., "Probability of Motor Failures Due to Environmental Effects," Technological Consultants, Inc., Redstone Arsenal, T-CR-78-11, March 1978.

[13] Williams, M.L., Blatz, P.J., and Shapery, R.A., "Fundamental Studies Relating to Systems Analysis of Solid Propellants," California Institute of Technology, GALCIT, SM 61-5, 1961, pp. 165-166.

[14] "Solmet, Hourly Solar Radiation-Surface Meteorological Observations," U.S. Dept. of Commerce, National Oceanic and Atmospheric Administration Environmental Data Service, Ashville, N.C., WBAN No. 23183, 1977.